IJOER
RESEARCH JOURNAL

International Journal of Engineering Research & Science

ISSN
2395-6992

www.ijoer.com
www.adpublications.org

Volume-7! Issue-1! January, 2021 www.ijoer.com ! info@ijoer.com

Preface

We would like to present, with great pleasure, the inaugural volume-7, Issue-1, January 2021, of a scholarly journal, *International Journal of Engineering Research & Science*. This journal is part of the AD Publications series *in the field of Engineering, Mathematics, Physics, Chemistry and science Research Development*, and is devoted to the gamut of Engineering and Science issues, from theoretical aspects to application-dependent studies and the validation of emerging technologies.

This journal was envisioned and founded to represent the growing needs of Engineering and Science as an emerging and increasingly vital field, now widely recognized as an integral part of scientific and technical investigations. Its mission is to become a voice of the Engineering and Science community, addressing researchers and practitioners in below areas

Chemical Engineering	
Biomolecular Engineering	Materials Engineering
Molecular Engineering	Process Engineering
Corrosion Engineering	
Civil Engineering	
Environmental Engineering	Geotechnical Engineering
Structural Engineering	Mining Engineering
Transport Engineering	Water resources Engineering
Electrical Engineering	
Power System Engineering	Optical Engineering
Mechanical Engineering	
Acoustical Engineering	Manufacturing Engineering
Optomechanical Engineering	Thermal Engineering
Power plant Engineering	Energy Engineering
Sports Engineering	Vehicle Engineering
Software Engineering	
Computer-aided Engineering	Cryptographic Engineering
Teletraffic Engineering	Web Engineering
System Engineering	
Mathematics	
Arithmetic	Algebra
Number theory	Field theory and polynomials
Analysis	Combinatorics
Geometry and topology	Topology
Probability and Statistics	Computational Science
Physical Science	Operational Research
Physics	
Nuclear and particle physics	Atomic, molecular, and optical physics
Condensed matter physics	Astrophysics
Applied Physics	Modern physics
Philosophy	Core theories

Chemistry	
Analytical chemistry	Biochemistry
Inorganic chemistry	Materials chemistry
Neurochemistry	Nuclear chemistry
Organic chemistry	Physical chemistry
Other Engineering Areas	
Aerospace Engineering	Agricultural Engineering
Applied Engineering	Biomedical Engineering
Biological Engineering	Building services Engineering
Energy Engineering	Railway Engineering
Industrial Engineering	Mechatronics Engineering
Management Engineering	Military Engineering
Petroleum Engineering	Nuclear Engineering
Textile Engineering	Nano Engineering
Algorithm and Computational Complexity	Artificial Intelligence
Electronics & Communication Engineering	Image Processing
Information Retrieval	Low Power VLSI Design
Neural Networks	Plastic Engineering

Each article in this issue provides an example of a concrete industrial application or a case study of the presented methodology to amplify the impact of the contribution. We are very thankful to everybody within that community who supported the idea of creating a new Research with IJOER. We are certain that this issue will be followed by many others, reporting new developments in the Engineering and Science field. This issue would not have been possible without the great support of the Reviewer, Editorial Board members and also with our Advisory Board Members, and we would like to express our sincere thanks to all of them. We would also like to express our gratitude to the editorial staff of AD Publications, who supported us at every stage of the project. It is our hope that this fine collection of articles will be a valuable resource for *IJOER* readers and will stimulate further research into the vibrant area of Engineering and Science Research.

Mukesh Arora

(Chief Editor)

Dr. Mohamed Abdel Fatah Ashabrawy Moustafa

PhD. in Computer Science - Faculty of Science - Suez Canal University University, 2010, Egypt.

Assistant Professor Computer Science, Prince Sattam bin AbdulAziz University ALkharj, KSA.

Dr. Heba Mahmoud Mohamed Afify

Ph.D degree of philosophy in Biomedical Engineering, Cairo University, Egypt worked as Assistant Professor at MTI University.

Dr. Aurora Angela Pisano

Ph.D. in Civil Engineering, Currently Serving as Associate Professor of Solid and Structural Mechanics (scientific discipline area nationally denoted as ICAR/08"–"Scienza delle Costruzioni"), University Mediterranea of Reggio Calabria, Italy.

Dr. Faizullah Mahar

Associate Professor in Department of Electrical Engineering, Balochistan University Engineering & Technology Khuzdar. He is PhD (Electronic Engineering) from IQRA University, Defense View,Karachi, Pakistan.

Dr. S. Kannadhasan

Ph.D (Smart Antennas), M.E (Communication Systems), M.B.A (Human Resources).

Dr. Christo Ananth

Ph.D. Co-operative Networks, M.E. Applied Electronics, B.E Electronics & Communication Engineering Working as Associate Professor, Lecturer and Faculty Advisor/ Department of Electronics & Communication Engineering in Francis Xavier Engineering College, Tirunelveli.

Dr. S.R.Boselin Prabhu

Ph.D, Wireless Sensor Networks, M.E. Network Engineering, Excellent Professional Achievement Award Winner from Society of Professional Engineers Biography Included in Marquis Who's Who in the World (Academic Year 2015 and 2016). Currently Serving as Assistant Professor in the department of ECE in SVS College of Engineering, Coimbatore.

Dr. Maheshwar Shrestha

Postdoctoral Research Fellow in DEPT. OF ELE ENGG & COMP SCI, SDSU, Brookings, SD Ph.D, M.Sc. in Electrical Engineering from SOUTH DAKOTA STATE UNIVERSITY, Brookings, SD.

Zairi Ismael Rizman

Senior Lecturer, Faculty of Electrical Engineering, Universiti Teknologi MARA (UiTM) (Terengganu) Malaysia Master (Science) in Microelectronics (2005), Universiti Kebangsaan Malaysia (UKM), Malaysia. Bachelor (Hons.) and Diploma in Electrical Engineering (Communication) (2002), UiTM Shah Alam, Malaysia

Dr. D. Amaranatha Reddy

Ph.D.(Postdocteral Fellow,Pusan National University, South Korea), M.Sc., B.Sc. : Physics.

Dr. Dibya Prakash Rai

Post Doctoral Fellow (PDF), M.Sc.,B.Sc., Working as Assistant Professor in Department of Physics in Pachhuncga University College, Mizoram, India.

Dr. Pankaj Kumar Pal

Ph.D R/S, ECE Deptt., IIT-Roorkee.

Dr. P. Thangam

BE(Computer Hardware & Software), ME(CSE), PhD in Information & Communication Engineering, currently serving as Associate Professor in the Department of Computer Science and Engineering of Coimbatore Institute of Engineering and Technology.

Dr. Pradeep K. Sharma

PhD., M.Phil, M.Sc, B.Sc, in Physics, MBA in System Management, Presently working as Provost and Associate Professor & Head of Department for Physics in University of Engineering & Management, Jaipur.

Dr. R. Devi Priya

Ph.D (CSE),Anna University Chennai in 2013, M.E, B.E (CSE) from Kongu Engineering College, currently working in the Department of Computer Science and Engineering in Kongu Engineering College, Tamil Nadu, India.

Dr. Sandeep

Post-doctoral fellow, Principal Investigator, Young Scientist Scheme Project (DST-SERB), Department of Physics, Mizoram University, Aizawl Mizoram, India- 796001.

Mr. Abilash

MTech in VLSI, BTech in Electronics & Telecommunication engineering through A.M.I.E.T.E from Central Electronics Engineering Research Institute (C.E.E.R.I) Pilani, Industrial Electronics from ATI-EPI Hyderabad, IEEE course in Mechatronics, CSHAM from Birla Institute Of Professional Studies.

Mr. Varun Shukla

M.Tech in ECE from RGPV (Awarded with silver Medal By President of India), Assistant Professor, Dept. of ECE, PSIT, Kanpur.

Mr. Shrikant Harle

Presently working as a Assistant Professor in Civil Engineering field of Prof. Ram Meghe College of Engineering and Management, Amravati. He was Senior Design Engineer (Larsen & Toubro Limited, India).

Table of Contents

Volume-7, Issue-1, January 2021

Non-typical designs of Polypropylene Capillary Heat Exchangers

Mária Čarnogurská[1], Róbert Gallik[2]

Department of Power Engineering, Faculty of Mechanical Engineering, Technical University of Košice, 042 00 Košice, Slovak Republic

Received: 26 December 2020/ Revised: 6 January 2021/ Accepted: 12 January 2021/ Published: 31-01-2021

Abstract— *The present article describes a heat exchanger with transparent (smooth) fibres with an atypical body shape and an atypical arrangement of polypropylene capillaries inside. The exchanger cross-section was of a square shape. This type of exchanger was subjected to the investigation of the impact of the fibre arrangement on the overall heat transfer coefficient and behaviour of fibres during the experiment. The exchanger was examined in the counter flow arrangement. The exchanger with 1,400 transparent fibres with the outer diameter of 0.275 mm was examined at the secondary fluid flow rate of 150 $l\cdot h^{-1}$ to identify the overall heat transfer coefficient k which amounted to 520 $W\cdot m^{-2}\cdot K^{-1}$. When compared to an exchanger with identical parameters of fibres placed inside a cylindrical exchanger body, a decrease in the overall heat transfer coefficient represented 14%. At the flow rate of 200 $l\cdot h^{-1}$, the value of the overall heat transfer coefficient identified experimentally was 632 $W\cdot m^{-2}\cdot K^{-1}$. When compared to cylindrical exchanger with comparable fibre parameters, the value was 33% lower.*

Keywords— Heat exchangers, polypropylene fibres, typical designs Polypropylene Capillary.

I. INTRODUCTION

The use of polypropylene fibres in heat exchangers, the benefits of the used material, the production of fibres (capillaries) and sealing them in a potting were described by several authors, for example in papers [1-3]. It is a novel approach to designing exchangers with the heat-transfer surface consisting of polypropylene fibres with either an absolutely smooth and gas-proof surface, or a porous surface. The number of capillaries in a bundle placed inside a polyurethane tube with a diameter of ca 30 mm may range from several hundreds to thousands of pieces. It depends on a fibre diameter and a potting size, but primarily on the desired exchanger performance.

II. DESIGN DESCRIPTION

The parameters of the experimentally examined exchanger with a square cross-section are listed in Table 1. These parameters fully correspond with the experimentally examined heat exchanger with a circular cross-section described in paper [4]. A partial cross-section of the design of the analysed exchanger is shown in Fig. 1. A standard potting (1) of the bundle was inbuilt in the exchanger body (2). The bundle of fibres was intertwined between the partition plates (3). The heat exchanger body was made of PVC boards and steel screws. A red arrow indicates the inflow of the working medium into the exchanger. The medium flowed around the fibres in the bundle and through the openings in the partition plates across the entire exchanger. The positions and sizes of the openings in the partition plates were chosen randomly to improve the flow of the medium around the fibres. A blue arrow indicates the outflow of the working medium flowing inside the fibres.

TABLE 1
TECHNICAL PARAMETERS OF THE EXAMINED BUNDLE OF CAPILLARIES

Parameter	Value	Size
Number of fibres	1,400	pc
Length of fibres	680	mm
Outer diameter of fibres	0.275	mm
Heat-transfer surface area	0.822	m^2
Material of capillaries	polypropylene	-
Material of potting	polyurethane	-

In the space between the body and the partition plates, the fibres were fixed using a silicon sealant with the aim to fix them along the entire width of the partition plate and avoid fibre clustering. A view inside the analysed exchanger is shown in Fig. 2.

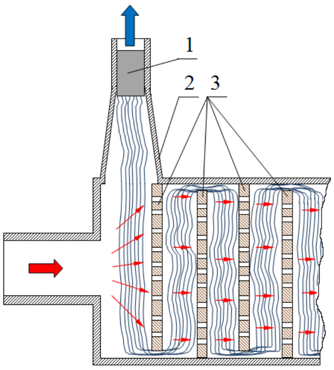

FIGURE 1: A cross-section of the square-shaped exchanger

FIGURE 2: A view inside the exchanger

III. RESULTS OF THE EXPERIMENTAL RESEARCH

The experiment preparation is documented in Fig. 3 which shows the procedure of installing individual fibres and partition plates into the exchanger body. The examined exchanger was attached to a measurement stand (Fig. 4) used in the experiment. The fibres in the bundle were filled with water from the distribution network and water flowing around the fibres was supplied from an accumulation tank.

The measurements were carried out by applying the standard procedure. Prior to the experiment, the fibres were subjected to a tightness test [5]. It was aimed at ensuring a faultless course of the measurements of temperatures and flow rates. Subsequently, the bundle was placed inside the exchanger body. After the exchanger was attached to the measurement stand, the tightness test was repeated [6] in order to exclude potential damage to the bundle caused by putting it inside the exchanger body. Following an inspection of the performance of the gauges (pressure meters, flow rate meters, thermometers), the flow rate of water flowing inside the fibres was set.

FIGURE 3: Procedure of installing fibres and partition plates

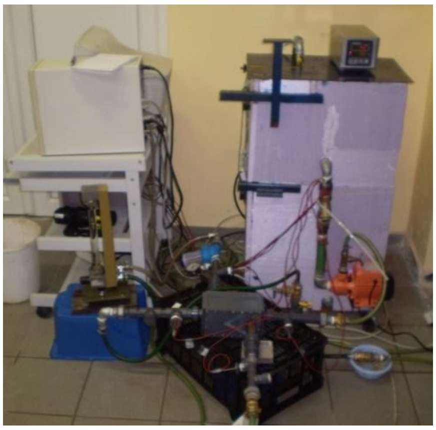

FIGURE 4: The exchanger during the measurements

A maximum flow rate value measured in the second tightness test was 200 $l \cdot h^{-1}$. During the measurements, the flow rate range from 30 $l \cdot h^{-1}$ to 200 $l \cdot h^{-1}$ was divided into five intervals (30 $l \cdot h^{-1}$; 60 $l \cdot h^{-1}$; 100 $l \cdot h^{-1}$; 150 $l \cdot h^{-1}$; and 200 $l \cdot h^{-1}$). Subsequently, the measurements were carried out from the lowest to the highest flow rate value. Water used in the experiment was supplied from the municipal distribution network. A temperature of water was constant during the entire experiment. The water pressure during the measurements was ca 400 kPa and it sufficiently covered the pressure loss of a single filter and flow rate meter which were installed in the inlet piping. After the parameters of water flowing through the bundle were stabilised, a water pump was used to force water around the fibres. The water was prepared in an external tank insulated on its external surface to avoid a heat loss. Water was heated by a 3 kW electric spiral. After the water circulation around the fibres was activated, temperatures were automatically measured by the computer software and displayed directly from a data logger on a computer screen. The whole process was visually monitored and as soon as the state was stabilised, i.e. when the measured parameters stopped exhibiting changes, a water flow regulation valve was used at the inlet into the bundle to set a new flow rate value for the water flowing inside the capillaries, i.e. in the secondary circuit of the exchanger. After the equilibrium state was reached, the flow rate was repeatedly adjusted to a higher value. The procedure was repeated until the flow rate of 200 $l \cdot h^{-1}$ was achieved. The time interval in which the equilibrium state was reached ranged from 3 to 5 minutes. In order to exclude potential technical failures of the used gauges, after reaching the steady state at the maximum flow rate of 200 $l \cdot h^{-1}$, the flow rate was gradually reduced in the same increments. After the measurements were completed, the recorded values of the measured parameters were further processed in a spreadsheet. The overall heat transfer coefficient was calculated using the formula (2). The number and length of fibres and their outer diameter were used to identify the heat transfer surface area. The size of this area is stated in Table 1.

Maximum thermal capacity of the exchanger was calculated using the following formula (1): [2]

$$P = k \cdot \overline{\Delta T} \cdot S = Q_{m2} \cdot c_p \cdot \left(T_2'' - T_2'\right) \text{ (W)} \tag{1}$$

Where in k is the overall heat transfer coefficient ($W \cdot m^{-2} \cdot K^{-1}$); $\overline{\Delta T}$ is the mean temperature gradient (K); Q_{m2} is the mass flow rate of water in the secondary circuit ($kg \cdot s^{-1}$); c_p is the specific heat capacity of water ($J \cdot kg^{-1} \cdot K^{-1}$); and S is the heat transfer surface area (m^2). T_2'' and T_2' are the temperatures of water in the secondary circuit at the inlet and outlet; T_1' and T_1'' are the temperatures of water in the primary circuit at the inlet and outlet.

The measured values of temperatures and flow rates may be used in the equation (1) to identify the overall heat transport coefficient, with the use of the equation (2). The following applies in general:

$$k = \frac{Q_{m2} \cdot c_p \cdot (T_2'' - T_2')}{\overline{\Delta T} \cdot S} \left(\mathrm{W \cdot m^{-2} \cdot K^{-1}}\right) \tag{2}$$

In the case of a counter flow exchanger, the mean temperature gradient was calculated using the following formula (3):

$$\overline{\Delta T} = \frac{(T_1' - T_2'') - (T_1'' - T_2')}{\ln \frac{T_1' - T_2''}{T_1'' - T_2'}} \tag{3}$$

A correlation between the overall heat transfer coefficient k and the flow rate in a partition plate heat exchanger with a square cross-section is shown in Fig. 5. Its maximum value was observed at the water flow rate inside the fibres of 200 $l \cdot h^{-1}$ and it amounted to as little as 630 $W \cdot m^{-2} \cdot K^{-1}$.

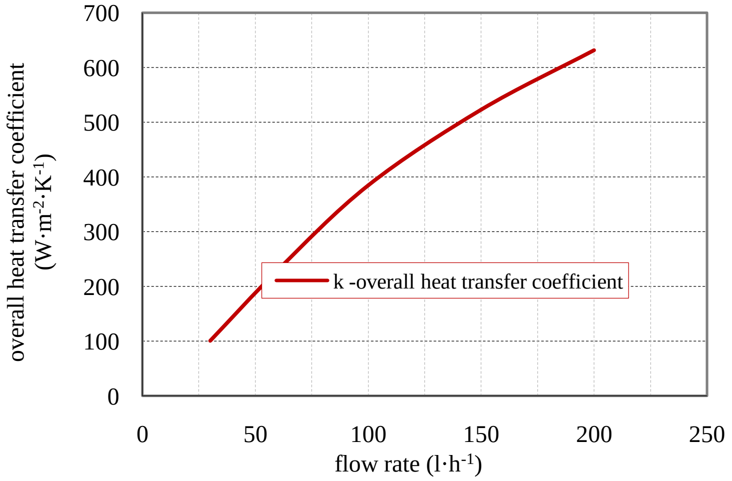

FIGURE 5: A correlation between the overall heat transfer coefficient and the flow rate

IV. CONCLUSION

An analysis of two different types of heat exchangers comprising polypropylene fibres with identical parameters showed that the heat transfer was more intensive in an exchanger with a circular body. This may be attributable to the fact that the fibres were forced against, and attached to, the wall (in a square-shaped exchanger body). At such places, the fibres were not sufficiently flown around by water (see Fig. 1), and such insufficient flow around the fibres was also observed in the entrance part of the exchanger - next to the potting. It is therefore possible to state that in this exchanger type a certain part of the fibres within their length practically did not contribute to the heat transfer. Removing this drawback in a square-shaped exchanger design might result in approximately a 20–25% increase in the value of the overall heat transfer coefficient. This analysis was based on a fictitious removal of the part of fibres which did not contribute to the heat transfer. As the fibres were forced against the wall, the heat-transfer surface area was in fact reduced.

A comparison of the results of the experimental identification of the value of the overall heat transfer coefficient in exchangers with circular or square external surface clearly indicated that higher intensity of the heat transfer may be achieved by using exchangers with cylindrical surfaces. As stated in the annotation of this article, at the maximum flow rate inside the fibres of 200 $l \cdot h^{-1}$, the square-shaped exchangers exhibited the value of the overall heat transfer coefficient which was lower in as much as 33%.

ACKNOWLEDGEMENTS

The paper has been produced as a part of a project KEGA 005TUKE-4/2019 and VEGA No. 1/0626/20.

REFERENCES

[1] D. M., Zarkadas, K. K. Sirkar, Polymeric Hollow Fiber Heat Exchangers: An Alternative for Lower. Temperature Applications. In Eng. Chem. Res., vol. 43, 2004, p. 8093-8106.

[2] M. Čarnogurská, R. Gallik, Special Types of Heat Exchangers, International Journal of Engineering Research & Science (IJOER) vol.6, 2020, p. 12-15.

[3] L., Jachuck, R. J. J. Zaheed, Review of polymer compact heat exchangers, with special emphasis on a polymer film unit. In Applied Thermal Engineering, vol. 24, 2004, no 16, p. 2323-2358.

[4] M. Čarnogurská, M.Příhoda, R. Gallik, Tthe impact of elementary structural parameters on the performance of heat exchanger made of polypropylene fibres, Materials and Technology, 54(6) 2020.

[5] R., Gallik, M. Dohnal, Potted sets of hollow fibers as low cost heat exchangers. (in Slovak). SROJÁRSTVO / SROJÍRENSTVÍ, (special edition). 2019, p. 61-62.

[6] K. Král, Technické merania. (in Slovak). Alfa, 2002, 155 s.

Voltage Control in Distribution System with Reactive Power Dispatch

Bharat Singh[1*], Jagnandan Negi[2], Satyaveer Singh Rawat[3]
Electrical Engineering Department, NIT Kurukshetra, Haryana, India
*Corresponding Author: Bharat Singh, Ph.D. Scholar, Electrical Engineering Department, NIT Kurukshetra, Haryana, India

Received: 24 December 2020/ Revised: 03 January 2021/ Accepted: 17 January 2021/ Published: 31-01-2021

Abstract— *Due to large resistance and lower reactance of lines, the voltage control and power loss became a crucial issue. The flat voltage profile, is therefore expected to distribution system at each node, minimum power loss, the maximum cost of saving and maximum efficiency. In this context, to find the size and location of compensating devices for the reactive power and voltage control devices became the essential need. In this paper, the multi-objective optimisation problem is solved for the sizing and location of reactive power compensating devices in the distribution system. The main contributions of the proposed work are*

(i) To address the hybrid algorithm to determine the location and size of Distribution Static Synchronous Compensator (D-STATCOM).

(ii) The power loss and voltage deviation are minimised.

(iii) The impact of D-STATCOM with minimum voltage growth is analysed.

The results are verified, tabulated and compared with other methods. The IEEE-33 bus test system has been taken for the analysis.

Keywords— Power loss minimisation, voltage deviation, D-STATCOM.

I. INTRODUCTION

The reactive power has been compensated using the capacitor banks, synchronous condenser, tap changers and voltage regulators etc, in the earlier distribution system. The optimal operation of the distribution network operator is comprised of the better voltage profile at each node, minimum power loss and higher cost of energy saving. The flat voltage profile is therefore expected to distribution system at each node, minimum power loss, the maximum cost of saving and maximum efficiency. One of the operations is to reactive power compensating devices which aims to manage the voltage control and reactive power control for minimisation of power loss.

The power loss has been reduced using the capacitor bank for power factor improvement also [1]. The active and reactive power has been compensated using the distribution generations and capacitor bank [2]. The meta-heuristic techniques are used to solve the reactive power dispatch problems [3]. In this context, the two-archive multi-objective grey wolf optimizer [4], modified differential evolution technique [5], multi-objective strategy [6], a combined swarming algorithm [7], gravitational search algorithm [8], learning based technique [9] etc., have been used for the reactive power dispatch. The uncertainty in renewable based generation has been implemented for reactive power dispatch, although the compensating devices were not used [10]. Apart from this, the distribution D-FACT devices have used to avoid the switching problem in capacitor bank for the reactive power dispatch and voltage control. The reactive power dispatch has been determined using the sitting of capacitor banks, tap position of tap changing transformers and generator voltage [11]. However the penalty based optimization problem has also been considered for the reactive power dispatch [12]. Apart from the above literature, the D-STATCOM has been used instead of capacitor bank for the reactive power dispatch and voltage control. In this context, the probabilistic assessments have been used for the D-STATCOM installation [13]. The D-STATCOM has been installed for the economic load sharing also [14]. The D-STATCOM has been installed to mitigate the low voltage fluctuations in the distribution system [15]. The voltage instability problem has also been mitigates using the D-STATCOM [16]. The various optimization techniques have been implemented for the installation of the D-STATCOM [17], lightning search algorithm (LSA) [18], the direct load flow (DLF) approach in [19], cuckoo search algorithm (CSA) [20], Levy flights algorithm [20] etc.

As evidenced by the literature review, the proposed work aims to determine the size and location of D-STATCOM for minimising the power loss and voltage deviation. The key contribution of this work is as follows:

(i) Determine the location and size of D-STATCOM to obtain the optimal reactive power dispatch.

(ii) To propose the GAMS algorithm for solving the multi-objective problem,

(iii) The rating of D-STATCOM has also been considered with the multi-objective problem.

The present work has been tested in IEEE-33 bus test system of radial distribution (RDS). The results have been tabulated and compared with the other existing methods and techniques also.

In this paper, the total of five sections is represented. In section 2, the problem formulation and system modeling is represented. In section 3, the proposed algorithm is explained. In section 4, the results part is discussed. In the last section 5, the paper is concluded.

II. PROBLEM FORMULATION AND MATHEMATICAL MODEL

In this section, the problem formulation and the mathematical model have been explained as follows;

The multi-objective function has been carried out for the analysis. In:

Objective 1: power loss has been determined.

Objective 2: the voltage deviation has been minimised.

The optimal location of D_STATCOM is determined to minimise the cost of energy loss and voltage deviation, as explained in equation (1) and (2).

$$min\{f_1\} = \sum_k^T \sum_i^{nb} \sum_j^{nl} \left| P_{Loss,ij}^k \right| \tag{1}$$

$$min\{f_2\} = \sum_k^T \sum_i^{nb} \left| \frac{\left(V_o - V_i^k\right)}{V_o} \right| \times 100 \tag{2}$$

The following constraints are considered;

Power balance constraints are represented in eq. (3) and (4).

$$P_i^k = \left(Pg_i^k - Pd_{ZIP,i}^k\right) = V_i^k \sum_{j=1}^n V_j^k \left(G_{ij} \cos\left(\delta_i^k - \delta_j^k\right) + B_{ij} \sin\left(\delta_i^k - \delta_j^k\right)\right) \tag{3}$$

$$Q_i^k = \left(Qg_i^k - Qd_{ZIP,i}^k\right) = V_i^k \sum_{j=1}^{n} V_j^k \left(G_{ij}\, sin\left(\delta_i^k - \delta_j^k\right) - B_{ij}\, cos\left(\delta_i^k - \delta_j^k\right)\right) \tag{4}$$

$\forall\ i \in S_B \,\&\, k \in S_T$

Where the generated power Pg_i^k and Qg_i^k is represented in (5) and (6)

$$Pg_i^k = Pgrid_i^k + \sum_j^{nl} P_{Loss,ij}^k \tag{5}$$

$$Qg_i^k = Pgrid_i^k + Q_{DST,i}^k + \sum_j^{nl} Q_{Loss,ij}^k \tag{6}$$

D-STATCOM limits: this includes the maximum and minimum limits.

$$Q_{DSTmin,i}^k \leq Q_{DST,i}^k \leq Q_{DSTmax,i}^k \tag{7}$$

Power loss equation represents in (10): this includes the maximum power limit.

$$\left|P_{Loss,ij}^k\right| = \left|\sum_k^T \sum_i^{nb} G_{ij}^k \left\{(V_i^k)^2 + (V_i^k)^2 - 2V_i^k V_j^k \cdot cos\left(\delta_i^k - \delta_j^k\right)\right\}\right| \leq Pl_{max}^k \tag{8}$$

Limits for the generation: this includes the maximum and minimum limits.

$$P_{Gi}^{min} \leq Pg_i \leq P_{gi}^{max}, i \in S_G \tag{9}$$

$$Q_{gi}^{min} \leq Qg_i \leq Q_{gi}^{max}, i \in S_G \tag{10}$$

Voltage and load angle limit

$$V_{i,k}^{min} \leq V_i^k \leq V_{i,k}^{max}, i \in S_B \tag{11}$$

$$\delta_{min}{}_i^k \leq \delta_i^k \leq \delta_{max}{}_i^k, \tag{12}$$

$\forall i = 1,2 \ldots .nb$

Power factor limit of the system is limited by (15)

$$pf_i^{lo} \leq pf_i \leq pf_i^{up}, i \in S_B \tag{13}$$

III. ALGORITHM USED

In this section, the proposed algorithm has been explained as follows;

The MATLAB and GAMS have been carried out for solving the problem. The location and size of D-STATCOM is determined using NLP solver in GAMS. The following steps are used to solve the multi-objective problem.

Step 1: Read the test system bus and line data.

Step 2: Run the load flow program for 24-hrs and obtain the candidate node having the highest power loss and voltage deviation for D-STATCOM location. Save the candidate node.

Step 3: After obtaining the location of the candidate node, the size of D-STATCOM has determined. Transfer the all control parameter from MATLAB to GAMS.

Solve the objective function (1) and (2). Solve the constraints equation from (3) to (13).

Step 4: Transfer the objective variables form GAMS to MATLAB.

Step 5: Save and Print the results.

The flow chart of the proposed algorithm is shown in Figure 1.

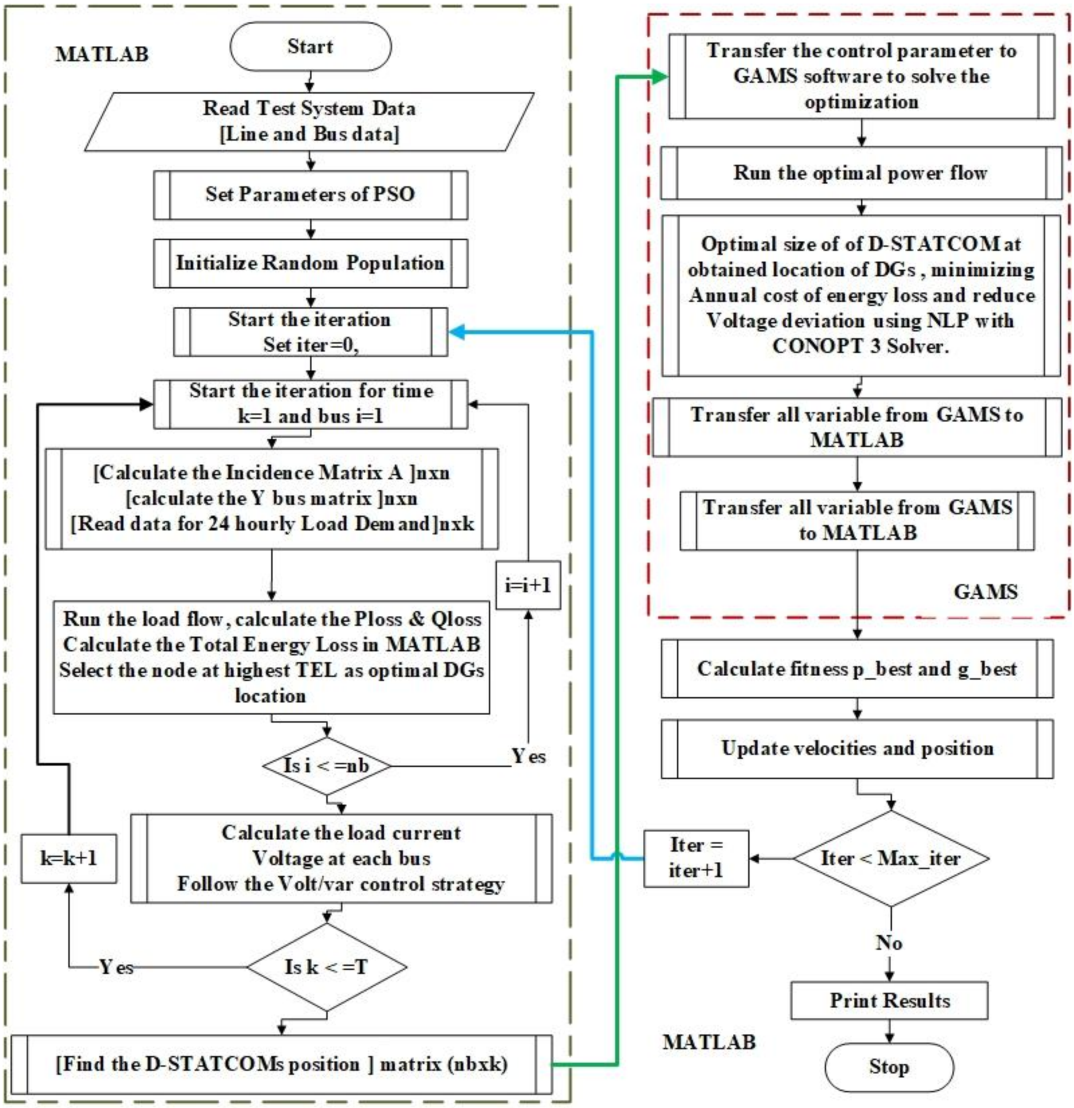

FIGURE 1: Flow chart for the proposed algorithm

IV. RESULT AND DISCUSSION

In this section, the simulation results have been presented and discussed to study the D-STATCOM in distribution system. Furthermore, the proposed technique has been tested on distribution system: 100 MVA 12.66 kV IEEE 33 bus test system. Moreover, the rating of D-STATCOM has been determined with minimum voltage growth from 0.90 to 0.95 pu for better reactive power sources to minimise the power loss. The rating of multiple D-STATCOM, power loss, annual cost of energy loss, and saving of energy loss have been analysed. The following cases have been carried out for the analysis as follows;

Case 1: The impact of single D-STATCOM.

Case 2: The impact of multiple D-STATCOM.

Case 3: The impact of time-varying ZIP load with D-STATCOM.

The test system has been carried out with the above mentioned cases.

4.1 Result for Test system 1: IEEE 33 bus test system

In this section, the D-STATCOM rating and location have been determined to obtain the reactive power dispatch and maximum energy saving in IEEE 33-bus system.

In the base case, the peak demand of the distribution system is 3715+j2300 kVA. The base case power loss is 202.66+j135.13 kVA annual cost of energy loss is $106518.1, and the minimum voltage is 0.9047930 pu.

4.1.1 Installation of D-STATCOM

The optimal location obtained for the single D-STATCOM is 30th bus, and the multiple D-STATCOM of two nodes is 12th and 30th, respectively. Furthermore, the rating of single D-STATCOM obtained is 1257.89 kVAr at 30th bus for power loss saving. The power loss obtained after installation of D-STATCOM is 145.3001+j*98.07289 kVA, the voltage profile has enhanced to 0.9245 pu, and the annual cost of energy loss obtained is $79365. Therefore, the saving in annual energy loss obtained is $23481.6 (28.303%).

In this context, the multiple D-STATCOM of 464.98 kVAr, and 1063.3 kVAr are installed at bus 12th and 30th, respectively. The power loss has been reduced to 136.1395+j*91.10344 kVA with multiple D-STATCOM. Therefore, the annual cost of energy loss obtained is $74359, and the annual saving in energy loss obtained is $36338 (32.827%). In Figure 2 the voltage profile with installation of D-STATCOM is shown.

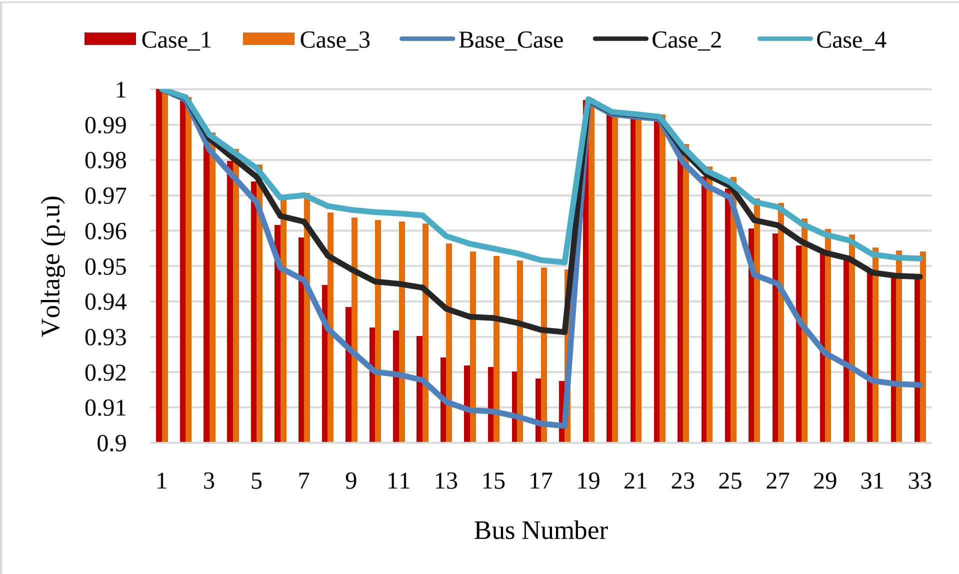

FIGURE 2: Minimum voltage profile with the installation of D-STATCOM in IEEE 33 bus system

TABLE 1
COMPARISON OF RESULTS FOR 33- BUS SYSTEM

Descriptions	Base Case	PSO [21]	BFOA [22]	LSF [19]	BAT [23]	IA [24]	GA [24]	Proposed with D-STATCOM
Optimal location at bus	------	30	30	30	30	12	12	30
Rating of D-STATCOM (kVAr)	------	1380	1102.7	3200	1150	962.49	1114.2	1257.89
Min. voltage (pu)	0.91309	0.92677	0.92422	0.9023	0.9244	0.9258	0.9236	0.9245
Total power loss (kW)	202.66	144.17	144.38	198.25	143.97	171.81	173.95	145.3
Loss reduction (%)	------	28.86	28.75	2.17	28.95	15.22	14.16	28.30
Total annual cost ($)	106518.1	83089.75	81730.44	121160.2	81765.63	95404.53	97333.38	83036.5
Cost of Compensation ($)		7314	5844.31	16960	6095	5101.197	5905.26	6666.817
Annual cost of energy loss ($)	106518.1	75775.75	75886.13	104200.2	75670.63	90303.34	91428.12	76369.68
Annual cost of energy loss saving ($)	0	23428.34	24787.66	-14642.1	24752.46	11113.56	9184.716	23481.6

The results have been compared with other existing methods and techniques as given in Table 1, the proposed method has shown better results with another method for the minimum power loss and voltage enhancement. Moreover, the power loss is reduced to 28.303%, and the minimum voltage is increased to 0.9245 pu with the proposed algorithm. Although, the size of D-STATCOM obtained is 1257.89kVAr for loss minimisation and voltage enhancement.

TABLE 2
COMPARISON OF RESULT OF MULTIPLE D-STATCOM IN 33 BUS SYSTEM

Descriptions	Base Case	PSO[21]	BFOA[22]	BAT[23]	Proposed with D-STATCOM
Optimal location at bus	------	12, 30	10, 30	10, 30	12, 30
Rating of D-STATCOM (kVAr)	------	472 (12) 1062 (30)	600 (10) 1200 (30)	450 (10) 995 (30)	464.98 (12) 1063.3 (30)
Total D-STATCOM (kVAr)		1534	1800	1445	1528.28
Min. voltage (pu)	0.91309	0.93636	0.9392	0.9356	0.9245
Total power loss (kW)	202.66	135.75	137.5	136.05	135.896
Loss reduction (%)	------	33.015	32.15	32.86	32.9438
Total annual cost ($)	106518.096	79480.4	81810	79166.38	79654.8052
Annual cost of energy loss ($)	106518.096	71350.2	72270	71507.88	71554.9212
Cost of compensation ($)	0	8130.2	9540	7658.5	8099.884
Annual cost of saving ($)	0	27037.696	24708.096	27351.716	26991.27

The power loss obtained is 135.896kW, the minimum voltage is 0.9245 pu, the annual cost of energy loss is $71554.92, with multiple D-STATCOM at bus 12 and 30, as given in Table I. Moreover, the D-STATCOM of 464.98 kVAr at 12 bus, and 1063.3 kVAr at 30th bus. The power loss is reduced to 32.94 %, with the proposed method is compared to another method.

V. CONCLUSION

It is observed that the proposed method has better results as compared with other techniques likewise PSO, LSF, BFOA, GA, and IA etc. The results are first analysed and compared with another technique considering D-STACOM only. In this context, the minimum voltage is obtained upto 0.95 pu with an optimal size of D-STATCOM and minimum power loss, by taking the D-STATCOM. Therefore, the following points concluded for the optimal solution of IEEE-33 bus test system are; the voltage deviation is reduced to 3.805 % form 5.456 % (base case), and power loss is reduced to 32.82% with multiple D-STATCOM. In the above-mentioned points the power loss and voltage deviation are reduced with D-STATCOM. Moreover, the voltage and power factor are remained within the limits. In addition, the new concept of D-STATCOM Therefore, the proposed approach has better results with other methods.

REFERENCES

[1] A. Chandra and T. Agarwal, "Capacitor Bank Designing for Power Factor Improvement," *Ijetae*, vol. 4, no. 8, pp. 235–239, 2014, doi: 10.1016/0957-4166(94)80092-8.

[2] S. Kansal, V. Kumar, and B. Tyagi, "Composite active and reactive power compensation of distribution networks," *2012 IEEE 7th Int. Conf. Ind. Inf. Syst. ICIIS 2012*, vol. 247667, pp. 1–6, 2012, doi: 10.1109/ICIInfS.2012.6304764.

[3] "Solution to optimal reactive power dispatch in transmission system using meta-heuristic techniques—Status and technological review.pdf." .

[4] K. Nuaekaew, P. Artrit, N. Pholdee, and S. Bureerat, "Optimal reactive power dispatch problem using a two-archive multi-objective grey wolf optimizer," *Expert Syst. Appl.*, vol. 87, pp. 79–89, 2017, doi: 10.1016/j.eswa.2017.06.009.

[5] S. Biswas Raha and N. Chakraborty, "Tuned reactive power dispatch through modified differential evolution technique," *Front. Energy*, vol. 6, no. 2, pp. 138–147, 2012, doi: 10.1007/s11708-012-0188-8.

[6] A. Ghasemi, K. Valipour, and A. Tohidi, "Multi objective optimal reactive power dispatch using a new multi objective strategy," *Int. J. Electr. Power Energy Syst.*, vol. 57, pp. 318–334, 2014, doi: 10.1016/j.ijepes.2013.11.049.

[7] S. M. Shareef and R. Srinivasa Rao, "Optimal reactive power dispatch under unbalanced conditions using hybrid swarm intelligence," *Comput. Electr. Eng.*, vol. 69, no. June, pp. 183–193, 2018, doi: 10.1016/j.compeleceng.2018.05.011.

[8] S. Duman, Y. Sönmez, U. Güvenç, and N. Yörükeren, "Optimal reactive power dispatch using a gravitational search algorithm," *IET Gener. Transm. Distrib.*, vol. 6, no. 6, pp. 563–576, 2012, doi: 10.1049/iet-gtd.2011.0681.

[9] M. Ghasemi, M. Taghizadeh, S. Ghavidel, J. Aghaei, and A. Abbasian, "Solving optimal reactive power dispatch problem using a

novel teaching-learning-based optimization algorithm,” *Eng. Appl. Artif. Intell.*, vol. 39, pp. 100–108, 2015, doi: 10.1016/j.engappai.2014.12.001.

[10] S. M. Mohseni-Bonab, A. Rabiee, and B. Mohammadi-Ivatloo, “Voltage stability constrained multi-objective optimal reactive power dispatch under load and wind power uncertainties: A stochastic approach,” *Renew. Energy*, vol. 85, pp. 598–609, 2016, doi: 10.1016/j.renene.2015.07.021.

[11] A. Rajan and T. Malakar, “Optimal reactive power dispatch using hybrid Nelder-Mead simplex based firefly algorithm,” *Int. J. Electr. Power Energy Syst.*, vol. 66, pp. 9–24, 2015, doi: 10.1016/j.ijepes.2014.10.041.

[12] E. M. Soler, E. N. Asada, and G. R. M. Da Costa, “Penalty-based nonlinear solver for optimal reactive power dispatch with discrete controls,” *IEEE Trans. Power Syst.*, vol. 28, no. 3, pp. 2174–2182, 2013, doi: 10.1109/TPWRS.2013.2252207.

[13] S. Rezaeian-Marjani, S. Masoumzadehasl, S. Galvani, and V. Talavat, “Probabilistic assessment of D-STATCOM operation considering correlated uncertain variables,” *Int. Trans. Electr. Energy Syst.*, vol. 30, no. 10, pp. 1–23, 2020, doi: 10.1002/2050-7038.12522.

[14] S. Choudhury, P. Bhowmik, and P. K. Rout, “Economic load sharing in a D-STATCOM Integrated Islanded Microgrid based on Fuzzy Logic and Seeker Optimization Approach,” *Sustain. Cities Soc.*, vol. 37, no. July 2017, pp. 57–69, 2018, doi: 10.1016/j.scs.2017.11.004.

[15] M. M. Aggarwal and P. S. K. Gupta, “D-STATCOM control in Low Voltage Distribution System with Distributed,” pp. 426–429, 2010, doi: 10.1109/ICETET.2010.148.

[16] I. N. Power, “Reactive Power Compensation using D-STATCOM with Fuzzy Logic Supervision,” pp. 1–6, 2016.

[17] V. V. S. N. Murty and A. Kumar, “Impact of D-STATCOM in distribution systems with load growth on stability margin enhancement and energy savings using PSO and GAMS,” *Int. Trans. Electr. Energy Syst.*, vol. 28, no. 11, pp. 1–24, 2018, doi: 10.1002/etep.2624.

[18] Y. Thangaraj and R. Kuppan, “Multi-objective simultaneous placement of DG and DSTATCOM using novel lightning search algorithm,” *J. Appl. Res. Technol.*, vol. 15, no. 5, pp. 477–491, 2017, doi: 10.1016/j.jart.2017.05.008.

[19] F. Iqbal, M. T. Khan, and A. S. Siddiqui, “Optimal placement of DG and DSTATCOM for loss reduction and voltage profile improvement,” *Alexandria Eng. J.*, vol. 57, no. 2, pp. 755–765, 2018, doi: 10.1016/j.aej.2017.03.002.

[20] M. Ghosh, S. Kumar, S. Mandal, and K. K. Mandal, “Optimal sizing and placement of DG units in radial distribution system using cuckoo search algorithm,” *Int. J. Appl. Eng. Res.*, vol. 12, no. Special Issue 1, pp. 362–369, 2017.

[21] S. Devi and M. Geethanjali, “Electrical Power and Energy Systems Optimal location and sizing determination of Distributed Generation and DSTATCOM using Particle Swarm Optimization algorithm,” *Int. J. Electr. POWER ENERGY Syst.*, vol. 62, pp. 562–570, 2014, doi: 10.1016/j.ijepes.2014.05.015.

[22] K. R. Devabalaji and K. Ravi, “Optimal size and siting of multiple DG and DSTATCOM in radial distribution system using Bacterial Foraging Optimization Algorithm,” *Ain Shams Eng. J.*, vol. 7, no. 3, pp. 959–971, 2016, doi: 10.1016/j.asej.2015.07.002.

[23] T. Yuvaraj, K. Ravi, and K. R. Devabalaji, “DSTATCOM allocation in distribution networks considering load variations using bat algorithm,” *Ain Shams Eng. J.*, vol. 8, no. 3, pp. 391–403, 2017, doi: 10.1016/j.asej.2015.08.006.

[24] S. A. Taher and S. A. Afsari, “Optimal location and sizing of DSTATCOM in distribution systems by immune algorithm,” *Int. J. Electr. Power Energy Syst.*, vol. 60, pp. 34–44, 2014, doi: 10.1016/j.ijepes.2014.02.020.

AD Publications

Sector-3, MP Nagar, Bikaner,
Rajasthan, India
www.adpublications.org, info@adpublications.org